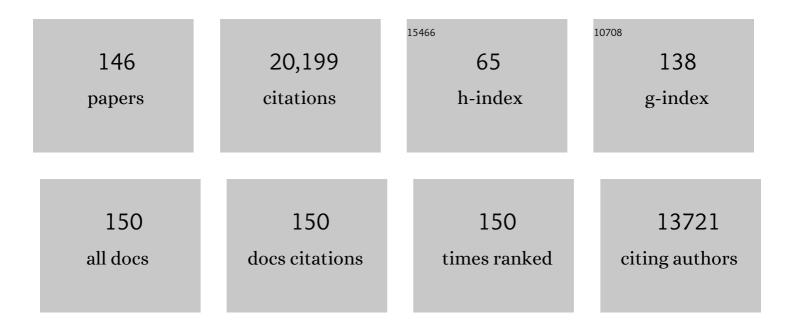
List of Publications by Year in descending order

Source: https://exaly.com/author-pdf/619209/publications.pdf Version: 2024-02-01



LUNUE ZHONG

#	Article	IF	CITATIONS
1	CO <sub>2</sub> electroreduction to ethylene via hydroxide-mediated copper catalysis at an abrupt interface. Science, 2018, 360, 783-787.	6.0	1,638
2	Enhanced electrocatalytic CO2 reduction via field-induced reagent concentration. Nature, 2016, 537, 382-386.	13.7	1,429
3	CO <sub>2</sub> electrolysis to multicarbon products at activities greater than 1 A cm <sup>â^2</sup> . Science, 2020, 367, 661-666.	6.0	860
4	Dopant-induced electron localization drives CO2 reduction to C2 hydrocarbons. Nature Chemistry, 2018, 10, 974-980.	6.6	781
5	Electrochemical CO <sub>2</sub> Reduction into Chemical Feedstocks: From Mechanistic Electrocatalysis Models to System Design. Advanced Materials, 2019, 31, e1807166.	11.1	769
6	Molecular tuning of CO2-to-ethylene conversion. Nature, 2020, 577, 509-513.	13.7	682
7	Enhanced Nitrate-to-Ammonia Activity on Copper–Nickel Alloys via Tuning of Intermediate Adsorption. Journal of the American Chemical Society, 2020, 142, 5702-5708.	6.6	638
8	CO <sub>2</sub> electrolysis to multicarbon products in strong acid. Science, 2021, 372, 1074-1078.	6.0	541
9	Steering post-C–C coupling selectivity enables high efficiency electroreduction of carbon dioxide to multi-carbon alcohols. Nature Catalysis, 2018, 1, 421-428.	16.1	537
10	Multi-site electrocatalysts for hydrogen evolution in neutral media by destabilization of water molecules. Nature Energy, 2019, 4, 107-114.	19.8	470
11	Turning the Page: Advancing Paper-Based Microfluidics for Broad Diagnostic Application. Chemical Reviews, 2017, 117, 8447-8480.	23.0	439
12	Cooperative CO2-to-ethanol conversion via enriched intermediates at molecule–metal catalyst interfaces. Nature Catalysis, 2020, 3, 75-82.	16.1	390
13	Efficient electrically powered CO2-to-ethanol via suppression of deoxygenation. Nature Energy, 2020, 5, 478-486.	19.8	363
14	Copper nanocavities confine intermediates for efficient electrosynthesis of C3 alcohol fuels from carbon monoxide. Nature Catalysis, 2018, 1, 946-951.	16.1	354
15	Binding Site Diversity Promotes CO <sub>2</sub> Electroreduction to Ethanol. Journal of the American Chemical Society, 2019, 141, 8584-8591.	6.6	338
16	Metal–Organic Frameworks Mediate Cu Coordination for Selective CO <sub>2</sub> Electroreduction. Journal of the American Chemical Society, 2018, 140, 11378-11386.	6.6	326
17	Catalyst synthesis under CO2 electroreduction favours faceting and promotes renewable fuels electrosynthesis. Nature Catalysis, 2020, 3, 98-106.	16.1	325
18	Copper-on-nitride enhances the stable electrosynthesis of multi-carbon products from CO2. Nature Communications, 2018, 9, 3828.	5.8	279

#	Article	IF	CITATIONS
19	Optofluidics for energy applications. Nature Photonics, 2011, 5, 583-590.	15.6	266
20	Magnetic Extraction of Microplastics from Environmental Samples. Environmental Science and Technology Letters, 2019, 6, 68-72.	3.9	242
21	High Rate, Selective, and Stable Electroreduction of CO <sub>2</sub> to CO in Basic and Neutral Media. ACS Energy Letters, 2018, 3, 2835-2840.	8.8	230
22	Constraining CO coverage on copper promotes high-efficiency ethylene electroproduction. Nature Catalysis, 2019, 2, 1124-1131.	16.1	214
23	Combined high alkalinity and pressurization enable efficient CO <sub>2</sub> electroreduction to CO. Energy and Environmental Science, 2018, 11, 2531-2539.	15.6	214
24	Designing anion exchange membranes for CO2 electrolysers. Nature Energy, 2021, 6, 339-348.	19.8	209
25	Hydroxide promotes carbon dioxide electroreduction to ethanol on copper via tuning of adsorbed hydrogen. Nature Communications, 2019, 10, 5814.	5.8	201
26	Photon management for augmented photosynthesis. Nature Communications, 2016, 7, 12699.	5.8	200
27	A Surface Reconstruction Route to High Productivity and Selectivity in CO <sub>2</sub> Electroreduction toward C <sub>2+</sub> Hydrocarbons. Advanced Materials, 2018, 30, e1804867.	11.1	200
28	2D Metal Oxyhalideâ€Derived Catalysts for Efficient CO <sub>2</sub> Electroreduction. Advanced Materials, 2018, 30, e1802858.	11.1	200
29	Chloride-mediated selective electrosynthesis of ethylene and propylene oxides at high current density. Science, 2020, 368, 1228-1233.	6.0	196
30	Efficient electrocatalytic conversion of carbon monoxide to propanol using fragmented copper. Nature Catalysis, 2019, 2, 251-258.	16.1	188
31	Deep Learning with Microfluidics for Biotechnology. Trends in Biotechnology, 2019, 37, 310-324.	4.9	160
32	Self-Cleaning CO <sub>2</sub> Reduction Systems: Unsteady Electrochemical Forcing Enables Stability. ACS Energy Letters, 2021, 6, 809-815.	8.8	159
33	High-Density Nanosharp Microstructures Enable Efficient CO <sub>2</sub> Electroreduction. Nano Letters, 2016, 16, 7224-7228.	4.5	158
34	Single Pass CO <sub>2</sub> Conversion Exceeding 85% in the Electrosynthesis of Multicarbon Products via Local CO <sub>2</sub> Regeneration. ACS Energy Letters, 2021, 6, 2952-2959.	8.8	155
35	Efficient Methane Electrosynthesis Enabled by Tuning Local CO <sub>2</sub> Availability. Journal of the American Chemical Society, 2020, 142, 3525-3531.	6.6	154
36	Copper adparticle enabled selective electrosynthesis of n-propanol. Nature Communications, 2018, 9, 4614.	5.8	153

JUNJIE ZHONG

#	Article	IF	CITATIONS
37	Pore-Scale Assessment of Nanoparticle-Stabilized CO <sub>2</sub> Foam for Enhanced Oil Recovery. Energy & Fuels, 2014, 28, 6221-6227.	2.5	150
38	Stable, active CO2 reduction to formate via redox-modulated stabilization of active sites. Nature Communications, 2021, 12, 5223.	5.8	145
39	Energy: the microfluidic frontier. Lab on A Chip, 2014, 14, 3127-3134.	3.1	144
40	Microfluidics for sperm analysis and selection. Nature Reviews Urology, 2017, 14, 707-730.	1.9	144
41	Hydronium-Induced Switching between CO <sub>2</sub> Electroreduction Pathways. Journal of the American Chemical Society, 2018, 140, 3833-3837.	6.6	144
42	Two-dimensional slither swimming of sperm within a micrometre of a surface. Nature Communications, 2015, 6, 8703.	5.8	135
43	Efficient upgrading of CO to C3 fuel using asymmetric C-C coupling active sites. Nature Communications, 2019, 10, 5186.	5.8	127
44	Optofluidic Concentration: Plasmonic Nanostructure as Concentrator and Sensor. Nano Letters, 2012, 12, 1592-1596.	4.5	121
45	Direct DNA Analysis with Paper-Based Ion Concentration Polarization. Journal of the American Chemical Society, 2015, 137, 13913-13919.	6.6	121
46	Tuning OH binding energy enables selective electrochemical oxidation of ethylene to ethylene glycol. Nature Catalysis, 2020, 3, 14-22.	16.1	120
47	Fluorescent Dyes for Visualizing Microplastic Particles and Fibers in Laboratory-Based Studies. Environmental Science and Technology Letters, 2019, 6, 334-340.	3.9	115
48	Oxygen-tolerant electroproduction of C <sub>2</sub> products from simulated flue gas. Energy and Environmental Science, 2020, 13, 554-561.	15.6	113
49	High-Rate and Efficient Ethylene Electrosynthesis Using a Catalyst/Promoter/Transport Layer. ACS Energy Letters, 2020, 5, 2811-2818.	8.8	106
50	CO <sub>2</sub> Electroreduction to Formate at a Partial Current Density of 930 mA cm <sup>–2</sup> with InP Colloidal Quantum Dot Derived Catalysts. ACS Energy Letters, 2021, 6, 79-84.	8.8	100
51	Low coordination number copper catalysts for electrochemical CO2 methanation in a membrane electrode assembly. Nature Communications, 2021, 12, 2932.	5.8	97
52	Efficient electrosynthesis of n-propanol from carbon monoxide using a Ag–Ru–Cu catalyst. Nature Energy, 2022, 7, 170-176.	19.8	96
53	Carbon-efficient carbon dioxide electrolysers. Nature Sustainability, 2022, 5, 563-573.	11.5	95
54	Promoting CO2 methanation via ligand-stabilized metal oxide clusters as hydrogen-donating motifs. Nature Communications, 2020, 11, 6190.	5.8	93

#	Article	IF	CITATIONS
55	Silica-copper catalyst interfaces enable carbon-carbon coupling towards ethylene electrosynthesis. Nature Communications, 2021, 12, 2808.	5.8	91
56	Suppressing the liquid product crossover in electrochemical CO <sub>2</sub> reduction. SmartMat, 2021, 2, 12-16.	6.4	90
57	Field-emission from quantum-dot-in-perovskite solids. Nature Communications, 2017, 8, 14757.	5.8	83
58	Microfluidic and nanofluidic phase behaviour characterization for industrial CO <sub>2</sub> , oil and gas. Lab on A Chip, 2017, 17, 2740-2759.	3.1	83
59	Rapid Microfluidics-Based Measurement of CO <sub>2</sub> Diffusivity in Bitumen. Energy & Fuels, 2011, 25, 4829-4835.	2.5	82
60	Steam-on-a-chip for oil recovery: the role of alkaline additives in steam assisted gravity drainage. Lab on A Chip, 2013, 13, 3832.	3.1	81
61	Full Characterization of CO <sub>2</sub> –Oil Properties On-Chip: Solubility, Diffusivity, Extraction Pressure, Miscibility, and Contact Angle. Analytical Chemistry, 2018, 90, 2461-2467.	3.2	78
62	In Situ Formation of Nano Ni–Co Oxyhydroxide Enables Water Oxidation Electrocatalysts Durable at High Current Densities. Advanced Materials, 2021, 33, e2103812.	11.1	78
63	Deep learning for the classification of human sperm. Computers in Biology and Medicine, 2019, 111, 103342.	3.9	73
64	Enhanced multi-carbon alcohol electroproduction from CO via modulated hydrogen adsorption. Nature Communications, 2020, 11, 3685.	5.8	72
65	Gold-in-copper at low *CO coverage enables efficient electromethanation of CO2. Nature Communications, 2021, 12, 3387.	5.8	70
66	Fast Fluorescence-Based Microfluidic Method for Measuring Minimum Miscibility Pressure of CO <sub>2</sub> in Crude Oils. Analytical Chemistry, 2015, 87, 3160-3164.	3.2	68
67	Capillary Condensation in 8 nm Deep Channels. Journal of Physical Chemistry Letters, 2018, 9, 497-503.	2.1	65
68	Bitumen–Toluene Mutual Diffusion Coefficients Using Microfluidics. Energy & Fuels, 2013, 27, 2042-2048.	2.5	64
69	Deep learning-based selection of human sperm with high DNA integrity. Communications Biology, 2019, 2, 250.	2.0	64
70	Paper-Based Quantification of Male Fertility Potential. Clinical Chemistry, 2016, 62, 458-465.	1.5	60
71	Joint tuning of nanostructured Cu-oxide morphology and local electrolyte programs high-rate CO <sub>2</sub> reduction to C <sub>2</sub> H <sub>4</sub> . Green Chemistry, 2017, 19, 4023-4030.	4.6	58
72	Nanomodel visualization of fluid injections in tight formations. Nanoscale, 2018, 10, 21994-22002.	2.8	56

#	Article	IF	CITATIONS
73	A glucose meter interface for point-of-care gene circuit-based diagnostics. Nature Communications, 2021, 12, 724.	5.8	54
74	Downstream of the CO <sub>2</sub> Electrolyzer: Assessing the Energy Intensity of Product Separation. ACS Energy Letters, 2021, 6, 4405-4412.	8.8	53
75	Condensation in One-Dimensional Dead-End Nanochannels. ACS Nano, 2017, 11, 304-313.	7.3	52
76	Accessory-free quantitative smartphone imaging of colorimetric paper-based assays. Lab on A Chip, 2019, 19, 1991-1999.	3.1	52
77	Increased Temperature and Turbulence Alter the Effects of Leachates from Tire Particles on Fathead Minnow ( <i>Pimephales promelas</i> ). Environmental Science & Technology, 2020, 54, 1750-1759.	4.6	52
78	Direct and Indirect Electroosmotic Flow Velocity Measurements in Microchannels. Journal of Colloid and Interface Science, 2002, 254, 184-189.	5.0	51
79	Microfluidic Manufacturing of Polymeric Nanoparticles: Comparing Flow Control of Multiscale Structure in Single-Phase Staggered Herringbone and Two-Phase Reactors. Langmuir, 2016, 32, 12781-12789.	1.6	48
80	Bubble nucleation and growth in nanochannels. Physical Chemistry Chemical Physics, 2017, 19, 8223-8229.	1.3	48
81	Biological Responses to Climate Change and Nanoplastics Are Altered in Concert: Full-Factor Screening Reveals Effects of Multiple Stressors on Primary Producers. Environmental Science & Technology, 2020, 54, 2401-2410.	4.6	48
82	Disposable silicon-glass microfluidic devices: precise, robust and cheap. Lab on A Chip, 2018, 18, 3872-3880.	3.1	47
83	Microfluidic pore-scale comparison of alcohol- and alkaline-based SAGD processes. Journal of Petroleum Science and Engineering, 2017, 154, 139-149.	2.1	46
84	Nanoscale Phase Measurement for the Shale Challenge: Multicomponent Fluids in Multiscale Volumes. Langmuir, 2018, 34, 9927-9935.	1.6	45
85	Determination of Dew Point Conditions for CO <sub>2</sub> with Impurities Using Microfluidics. Environmental Science & Technology, 2014, 48, 3567-3574.	4.6	44
86	Exploring Anomalous Fluid Behavior at the Nanoscale: Direct Visualization and Quantification via Nanofluidic Devices. Accounts of Chemical Research, 2020, 53, 347-357.	7.6	43
87	Low pressure supercritical CO2 extraction of astaxanthin from Haematococcus pluvialis demonstrated on a microfluidic chip. Bioresource Technology, 2018, 250, 481-485.	4.8	42
88	Predominance of sperm motion in corners. Scientific Reports, 2016, 6, 26669.	1.6	41
89	Asphaltene Deposition during Bitumen Extraction with Natural Gas Condensate and Naphtha. Energy & Fuels, 2018, 32, 1433-1439.	2.5	41
90	CO <sub>2</sub> Electroreduction to Methane at Production Rates Exceeding 100 mA/cm <sup>2</sup> . ACS Sustainable Chemistry and Engineering, 2020, 8, 14668-14673.	3.2	41

#	Article	IF	CITATIONS
91	Direct Visualization of Evaporation in a Two-Dimensional Nanoporous Model for Unconventional Natural Gas. ACS Applied Nano Materials, 2018, 1, 1332-1338.	2.4	40
92	Redox-mediated electrosynthesis of ethylene oxide from CO2 and water. Nature Catalysis, 2022, 5, 185-192.	16.1	40
93	Enhanced Solarâ€ŧoâ€Hydrogen Generation with Broadband Epsilonâ€Nearâ€Zero Nanostructured Photocatalysts. Advanced Materials, 2017, 29, 1701165.	11.1	39
94	Machine learning for sperm selection. Nature Reviews Urology, 2021, 18, 387-403.	1.9	39
95	Visualization and numerical modelling of microfluidic on-chip injection processes. Journal of Colloid and Interface Science, 2003, 260, 431-439.	5.0	38
96	A dynamic loading method for controlling on-chip microfluidic sample injection. Journal of Colloid and Interface Science, 2003, 266, 448-456.	5.0	38
97	Microfluidic assessment of swimming media for motility-based sperm selection. Biomicrofluidics, 2015, 9, 044113.	1.2	37
98	Eliminating the need for anodic gas separation in CO2 electroreduction systems via liquid-to-liquid anodic upgrading. Nature Communications, 2022, 13, .	5.8	37
99	Glycerol Oxidation Pairs with Carbon Monoxide Reduction for Low-Voltage Generation of C <sub>2</sub> and C <sub>3</sub> Product Streams. ACS Energy Letters, 2021, 6, 3538-3544.	8.8	36
100	Pore-scale analysis of steam-solvent coinjection: azeotropic temperature, dilution and asphaltene deposition. Fuel, 2018, 220, 151-158.	3.4	34
101	Visualization of fracturing fluid dynamics in a nanofluidic chip. Journal of Petroleum Science and Engineering, 2018, 165, 181-186.	2.1	33
102	Self-adaptive Bioinspired Hummingbird-wing Stimulated Triboelectric Nanogenerators. Scientific Reports, 2017, 7, 17143.	1.6	32
103	Light dilution via wavelength management for efficient highâ€density photobioreactors. Biotechnology and Bioengineering, 2017, 114, 1160-1169.	1.7	30
104	Natural gas vaporization in a nanoscale throat connected model of shale: multi-scale, multi-component and multi-phase. Lab on A Chip, 2019, 19, 272-280.	3.1	30
105	Microfluidic Synthesis of Photoresponsive Spool-Like Block Copolymer Nanoparticles: Flow-Directed Formation and Light-Triggered Dissociation. Chemistry of Materials, 2015, 27, 8094-8104.	3.2	29
106	FertDish: microfluidic sperm selection-in-a-dish for intracytoplasmic sperm injection. Lab on A Chip, 2021, 21, 775-783.	3.1	29
107	Field tested milliliter-scale blood filtration device for point-of-care applications. Biomicrofluidics, 2013, 7, 44111.	1.2	28
108	Biomass-to-biocrude on a chip via hydrothermal liquefaction of algae. Lab on A Chip, 2016, 16, 256-260.	3.1	27

#	Article	IF	CITATIONS
109	When robotics met fluidics. Lab on A Chip, 2020, 20, 709-716.	3.1	27
110	Dopant-tuned stabilization of intermediates promotes electrosynthesis of valuable C3 products. Nature Communications, 2019, 10, 4807.	5.8	26
111	Direct Measurement of the Fluid Phase Diagram. Analytical Chemistry, 2016, 88, 6986-6989.	3.2	25
112	Hydrothermal disruption of algae cells for astaxanthin extraction. Green Chemistry, 2017, 19, 106-111.	4.6	25
113	Culturing photosynthetic bacteria through surface plasmon resonance. Applied Physics Letters, 2012, 101, .	1.5	24
114	Nanoplastic State and Fate in Aquatic Environments: Multiscale Modeling. Environmental Science & Technology, 2022, 56, 4017-4028.	4.6	24
115	Prediction of DNA Integrity from Morphological Parameters Using a Single‣perm DNA Fragmentation Index Assay. Advanced Science, 2019, 6, 1900712.	5.6	23
116	A photosynthetic-plasmonic-voltaic cell: Excitation of photosynthetic bacteria and current collection through a plasmonic substrate. Applied Physics Letters, 2014, 104, 043704.	1.5	22
117	Self-assembled nanoparticle-stabilized photocatalytic reactors. Nanoscale, 2016, 8, 2107-2115.	2.8	22
118	Direct visualization of fluid dynamics in sub-10 nm nanochannels. Nanoscale, 2017, 9, 9556-9561.	2.8	22
119	Bubble Point Pressures of Hydrocarbon Mixtures in Multiscale Volumes from Density Functional Theory. Langmuir, 2018, 34, 14058-14068.	1.6	22
120	Effects of Hydrogen Peroxide on Cyanobacterium <i>Microcystis aeruginosa</i> in the Presence of Nanoplastics. ACS ES&T Water, 2021, 1, 1596-1607.	2.3	22
121	A combined method for pore-scale optical and thermal characterization of SAGD. Journal of Petroleum Science and Engineering, 2016, 146, 866-873.	2.1	21
122	Paper-based sperm DNA integrity analysis. Analytical Methods, 2016, 8, 6260-6264.	1.3	21
123	Screening High-Temperature Foams with Microfluidics for Thermal Recovery Processes. Energy & Fuels, 2021, 35, 7866-7873.	2.5	21
124	Digestible Fluorescent Coatings for Cumulative Quantification of Microplastic Ingestion. Environmental Science and Technology Letters, 2018, 5, 62-67.	3.9	19
125	Effects of liquid conductivity differences on multi-component sample injection, pumping and stacking in microfluidic chips. Lab on A Chip, 2003, 3, 173.	3.1	18
126	Gold Adparticles on Silver Combine Low Overpotential and High Selectivity in Electrochemical CO <sub>2</sub> Conversion. ACS Applied Energy Materials, 2021, 4, 7504-7512.	2.5	18

#	Article	IF	CITATIONS
127	Microplastics shift impacts of climate change on a plant-microbe mutualism: Temperature, CO2, and tire wear particles. Environmental Research, 2022, 203, 111727.	3.7	18
128	Disposable Plasmonics: Rapid and Inexpensive Large Area Patterning of Plasmonic Structures with CO <sub>2</sub> Laser Annealing. Langmuir, 2015, 31, 5252-5258.	1.6	16
129	Selection of high-quality sperm with thousands of parallel channels. Lab on A Chip, 2021, 21, 2464-2475.	3.1	15
130	Concentrated Ethanol Electrosynthesis from CO <sub>2</sub> via a Porous Hydrophobic Adlayer. ACS Applied Materials & Interfaces, 2022, 14, 4155-4162.	4.0	15
131	Breathable waveguides for combined light and CO2 delivery to microalgae. Bioresource Technology, 2016, 209, 391-396.	4.8	13
132	Fluorescence in sub-10 nm channels with an optical enhancement layer. Lab on A Chip, 2018, 18, 568-573.	3.1	13
133	The Full Pressure–Temperature Phase Envelope of a Mixture in 1000 Microfluidic Chambers. Angewandte Chemie - International Edition, 2017, 56, 13962-13967.	7.2	12
134	Accelerating Fluid Development on a Chip for Renewable Energy. Energy & Fuels, 2020, 34, 11219-11226.	2.5	10
135	Evaluation of a Microencapsulated Phase Change Slurry for Subsurface Energy Recovery. Energy & Fuels, 2021, 35, 10293-10302.	2.5	10
136	Past, Present, and Future of Microfluidic Fluid Analysis in the Energy Industry. Energy & Fuels, 2022, 36, 8578-8590.	2.5	10
137	Toxicity of nanoplastics to zooplankton is influenced by temperature, salinity, and natural particulate matter. Environmental Science: Nano, 2022, 9, 2678-2690.	2.2	10
138	Fiber refractometer to detect and distinguish carbon dioxide and methane leakage in the deep ocean. International Journal of Greenhouse Gas Control, 2014, 31, 41-47.	2.3	9
139	Band-aligned C <sub>3</sub> N <sub>4â^'x</sub> S <sub>3x/2</sub> stabilizes CdS/CuInGaS <sub>2</sub> photocathodes for efficient water reduction. Journal of Materials Chemistry A, 2017, 5, 3167-3171.	5.2	9
140	Periodic harvesting of microalgae from calcium alginate hydrogels for sustained highâ€density production. Biotechnology and Bioengineering, 2017, 114, 2023-2031.	1.7	9
141	The Full Pressure–Temperature Phase Envelope of a Mixture in 1000 Microfluidic Chambers. Angewandte Chemie, 2017, 129, 14150-14155.	1.6	6
142	How to select ICSI-viable sperm from the most challenging samples. Nature Reviews Urology, 2021, , .	1.9	3
143	AbCellera's success is unprecedented: what have we learned?. Lab on A Chip, 2021, 21, 2330-2332.	3.1	2
144	Frontispiz: The Full Pressure–Temperature Phase Envelope of a Mixture in 1000 Microfluidic Chambers. Angewandte Chemie, 2017, 129, .	1.6	1

#	Article	IF	CITATIONS
145	Inside Front Cover: Volume 2 Issue 1. SmartMat, 2021, 2, iii.	6.4	1
146	Frontispiece: The Full Pressure–Temperature Phase Envelope of a Mixture in 1000 Microfluidic Chambers. Angewandte Chemie - International Edition, 2017, 56, .	7.2	0